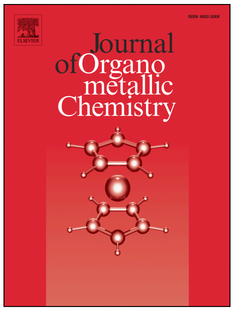

Syntheses, characterization and reactivity of dinuclear ruthenium-nickel complexes with hexane-2,5-dione bis(thiosemicarbazonato) ligands

Duo-Wen Fang, Ai-Quan Jia, Xian-Ping Dong, Zhifeng Xin, Qian-Feng Zhang

PII: S0022-328X(18)30300-0

DOI: 10.1016/j.jorganchem.2018.07.006

Reference: JOM 20493

To appear in: *Journal of Organometallic Chemistry*

Received Date: 3 May 2018

Revised Date: 3 July 2018

Accepted Date: 6 July 2018

Please cite this article as: D.-W. Fang, A.-Q. Jia, X.-P. Dong, Z. Xin, Q.-F. Zhang, Syntheses, characterization and reactivity of dinuclear ruthenium-nickel complexes with hexane-2,5-dione bis(thiosemicarbazonato) ligands, *Journal of Organometallic Chemistry* (2018), doi: 10.1016/j.jorganchem.2018.07.006.

Syntheses, characterization and reactivity of dinuclear ruthenium-nickel complexes with hexane-2,5-dione bis(thiosemicarbazonato) ligands

Duo-Wen Fang, Ai-Quan Jia*, Xian-Ping Dong, Zhifeng Xin, and Qian-Feng Zhang*

Institute of Molecular Engineering and Applied Chemistry, Anhui University of Technology,
Ma'anshan, Anhui 243002, P. R. China

Abstract

Treatment of hexane-2,5-dione bis(thiosemicarbazones) ([CH_3–C{=N–NH–C(=S)–NHR}–CH_2]$_2$, R = H, L^1H_2; CH_3, L^2H_2–Me; CH_2CH_3, L^3H_2–Et; C_6H_5, L^4H_2–Ph) with nickel(II) acetate hydrate in refluxing ethanol gave a series of $Ni^{II}N_2S_2$ metalloligands [Ni(L-R)] for the generation of hetero-bimetallic complexes. The reaction of equal mole each of [Ni(L^1)], [Ni(L^2–Me)], [Ni(L^3–Et)], or [Ni(L^4–Ph)] with [$RuCl_2$(dmso)$_4$] (dmso = dimethyl sulfoxide) at reflux resulted in isolation of neutral dinuclear ruthenium-nickel complexes [$RuCl_2${(Ni(L^1)}(dmso)$_2$] (**1**), [$RuCl_2${(Ni(L^2–Me)}(dmso)$_2$] (**2**), [$RuCl_2${(Ni(L^3–Et)}(dmso)$_2$] (**3**), and [$RuCl_2${(Ni(L^4–Ph)}(dmso)$_2$] (**4**). Interaction of [Ni(L-R)] with [CpRu(PPh_3)$_2$Cl] (Cp^- = cyclopentadienyl) at room temperature led to formation of cationic dinuclear organoruthenium-nickel complexes [CpRu{(Ni(L^1)}(PPh_3)]Cl (**5**), [CpRu{(Ni-(L^2–Me)}(PPh_3)]Cl (**6**), [CpRu{(Ni(L^3–Et}(PPh_3)]Cl (**7**), and [CpRu{(Ni(L^4–Ph}(PPh_3)]Cl (**8**). New bimetallic ruthenium-nickel complexes **1**–**8** have been characterized spectroscopically, of which molecular structures of three complexes [$RuCl_2${(Ni(L^2–Me)}(dmso)$_2$]·CH_2Cl_2 (**2**·CH_2Cl_2), [CpRu-{(Ni(L^2–Me)}(PPh_3)]Cl·EtOH (**6**·EtOH), and [CpRu{(Ni(L^3–Et}(PPh_3)]Cl (**7**·H_2O) have been established by single-crystal X-ray crystallography. Their catalytic activities for the acetalation of benzaldehyde in the presence of molecular H_2 have been also investigated in this paper.

Keywords: {Ni(μ-S)$_2$Ru}-type complex; Bis(thiosemicarbazones); Metalloligand; X-Ray crystal structure; Catalytic activity

---

* Corresponding authors. E-mails: jaiquan@ahut.edu.cn (A.-Q. Jia) and zhangqf@ahut.edu.cn (Q.-F. Zhang).

1. Introduction

Hydrogenases (H_2ases) are a class of biological enzymes which catalyze the production and consumption of molecular H_2 [1]. According to the metal content in their active sites, H_2ases are generally classified as [NiFe]H_2ases, [FeFe]H_2ases, and [Fe]H_2ases, of which [NiFe]H_2ases are the most popular and were firstly characterized by X-ray crystallography in 1995 [2]. Afterwards, the synthetic chemists have paid much attention on the designs and syntheses of various sulfur-bridged bimetallic [NiFe] complexes so that the catalytic mechanism of native [NiFe]H_2ases could be well understood [3–7]. As known, the elements of ruthenium and iron are congeners, of which the ruthenium atom may coordinate with both hard and soft ligands including dihydrogen or hydride. As a result, the preparation of bimetallic NiRu complexes to simulate the core structures of [NiFe]H_2ases has attracted great attention. In 2007, Ogo reported a NiRu-based bis(μ-thiolato)$Ni^{II}Ru^{II}$ complex, $[(NiL)Ru(H_2O)(\eta^6\text{-}C_6Me_6)](NO_3)_2$, which could catalyze the heterolytic cleavage of molecular H_2, successfully resulting in isolation of a hydrido bridged complex $[(Ni^{II}L)(H_2O)(\mu\text{-}H)Ru^{II}(\eta^6\text{-}C_6Me_6)](NO_3)$, where L = *N*,*N′*-dimethyl-*N*,*N′*-bis(2-mercaptoethyl)-1,3-propanediamine [8]. Moreover, several other organoruthenium-nickel complexes, based on $\{NiS_4\}$, $\{NiP_2S_2\}$, and $\{NiN_2S_2\}$ moieties, were synthesized in the following work and these complexes were shown to be capable of activation to the molecular H_2 [9–11]. On the other hand, the thiosemicarbazones functionalized groups with nitrogen and sulfur donor atoms may lead to various potent ligands by later modifications. These ligands and their transition metal complexes have been widely studied during past decades mainly due to their rich structure diversities and various biological properties [12, 13]. Thiosemicarbazones usually bond to transition metal ions through the sulfur and hydrazine nitrogen atoms to form four- or five-membered rings [14–16]. When referred to limited hexane-2,5-dione bis(thiosemicarbazonato) complexes, the stable 5:7:5-membered chelate ring systems accordingly formed [17–19]. Rauchfuss and Ogo have previously employed the nickel(II) metalloligands bearing flexible tetradentate N_2S_2 ligands, *N*,*N′*-dimethyl-*N*,*N′*-bis(2-mercaptoethyl)-1,3-diaminoethane, 1,5-bis(2-mercapto-2-methyl-propyl)-1,5-diazacyclooct-ane (bme*-daco), or *N*,*N′*-dimethyl-*N*,*N′*-bis(2-mercapto-ethyl)-1,3-propane-diamine, to construct bimetallic NiRu complexes [8, 20]. We have recently reported two organoruthenium-nickel complexes with a rigid tetradentate N_2S_2 ligand, *N*,*N*’-bis(2-thiobenzylidene)-1,2-phenylenediaminato, as shown in Chart 1 [21]. Herein, we describe the employment of a series of versatile and adjustable $\{NiN_2S_2\}$ metalloligands [Ni(L-R)] (L-R = hexane-2,5-dione bis(thiosemi-carbazonato)) to construct dinuclear ruthenium-nickel complexes. The reactivity of the structurally defined complexes towards molecular H_2 was initially investigated in this paper.

2. Experimental

2.1. General

All synthetic manipulations were carried out under dry dinitrogen atmosphere by standard Schlenk techniques. Solvents were purified, distilled and degassed prior to use. Published procedures were followed in the preparation of [Ni(L-R)] (L-R = hexane-2,5-dione bis(thiosemicarbazonato)) [17, 18], *cis*-[$RuCl_2$(dmso)$_4$] (dmso = dimethyl sulfoxide) [22], and [CpRu(PPh_3)$_2$Cl] (Cp^- = cyclopentadienyl) [23]. NMR spectra were recorded on a Bruker ALX 400 spectrometer operating at 400 and 162 MHz for ^1H and ^{31}P, respectively. Chemical shifts (δ, ppm) were reported with reference to $SiMe_4$ (^1H) and 85% H_3PO_4 (^{31}P). Infrared spectra (KBr) were recorded on a Perkin-Elmer 16 PC FT-IR spectrophotometer with use of pressed KBr pellets and positive FAB mass spectra were recorded on a Finnigan TSQ 7000 spectrometer. Elemental analyses were carried out using a Perkin-Elmer 2400 CHN analyzer. GC-MS experiments were performed on a Shimadzu GC-MS 2010 PLUS instrument.

*2.2. Preparation of [$RuCl_2${Ni(L^1)}(dmso)$_2$] (**1**)*

To a solution of [$RuCl_2$(dmso)$_4$] (48.5 mg, 0.10 mmol) in *N*,*N*-dimethyl formamide (DMF, 5 mL) was added a solution of [Ni(L^1)] (31.7 mg, 0.10 mmol) in DMF (5 mL), and then the mixture was stirred at reflux overnight, the resulting black solution was concentrated to ca. 3 mL. Slow addition of diethyl ether gave a black precipitate, which was filtered, washed by diethyl ether (3 × 5 mL) and hexane (3 × 5 mL), and dried under vacuum. Yield: 60 mg, 75% (based on Ru). IR (KBr disc, cm^{-1}): ν_{NH_2} 3454 (m); $\nu_{C=N}$ 1640 (m), 1608 (m); $\nu_{S=O}$ 1084 (s); $\nu_{C–S}$ 805 (m). ^1H NMR (400 MHz, DMSO-d_6): δ 8.78 (s, 2H, -NH_2), 8.70 (s, 2H, -NH_2), 3.60 (s, 3H, -CH_3S), 3.55 (s, 3H, -CH_3S), 3.48 (s, 3H, -CH_3S), 3.44 (s, 3H, -CH_3S), 3.35 (m, 2H, -CH_2), 2.84 (m, 2H, -CH_2), 1.95 (s, 3H, -CH_3), 1.89 (s, 3H, -CH_3) ppm. ^{13}C NMR (100 MHz, DMSO-d_6): 28.91 (CH_3), 29.23 (CH_3), 31.31 (CH_2), 31.35 (CH_2), 42.81 (SCH_3), 43.55 (SCH_3), 43.60 (SCH_3), 45.71 (SCH_3), 164.52 (*C*=N-N), 165.52 (*C*=N-N), 170.51 (N=*C*-S), 171.35 (N=*C*-S) ppm. FAB-MS (MeCN): *m*/*z* 574.4 [Ru{Ni(L^1)}(dmso)$_2$]$^+$, 496.2 [Ru{Ni(L^1)}(dmso)]$^+$, 418.1 [Ru{Ni(L^1)}]$^+$. *Anal*. Calcd. for $C_{12}H_{26}Cl_2N_6O_2S_4NiRu$: C, 22.34; H, 4.06; N, 13.02%. Found: C, 22.39; H, 4.04; N, 13.07%.

2.3. Preparation of $[RuCl_2\{Ni(L^2\text{-}Me)\}(dmso)_2]\cdot CH_2Cl_2$ (**2**$\cdot CH_2Cl_2$)

To a solution of $[RuCl_2(dmso)_4]$ (48.5 mg, 0.10 mmol) in tetrahydrofuran (THF, 5 mL) was added a solution of $[Ni(L^2\text{-}Me)]$ (34.5 mg, 0.10 mmol) in THF (10 mL), and then the mixture was stirred at reflux overnight, the resulting purple solution was concentrated to ca. 3 mL. Slow addition of diethyl ether gave a purple precipitate, which was filtered and washed by diethyl ether (3 × 5 mL) and hexane (3 × 5 mL). The product was then recrystallized from dichloromethane/diethyl ether to give black flake-shape crystals. Yield: 65 mg, 80% (based on Ru). IR (KBr disc, cm^{-1}): ν_{NH} 3254 (m); $\nu_{C=N}$ 1623 (m), 1600 (m); $\nu_{S=O}$ 1087 (s); $\nu_{C–S}$ 800 (m). ^1H NMR (400 MHz, $CDCl_3$): δ 7.46 (s, 1H, -N*H*), 6.39 (s, 1H, -N*H*), 3.57 (s, 3H, $-CH_3S$), 3.53 (s, 3H, $-CH_3S$), 3.42(m, 2H, $-CH_2$), 3.31 (s, 3H, $-CH_3S$), 3.04 (s, 3H, $-CH_3S$), 2.83 (d, *J* = 3.6 Hz, 6H, $-NHCH_3$), 2.43 (m, 2H, $-CH_2$), 2.07 (s, 3H, $-CH_3$), 2.04 (s, 3H, $-CH_3$) ppm. ^{13}C NMR (100 MHz, $CDCl_3$): 20.96 (CH_3), 21.42 (CH_3), 31.39 (CH_2), 31.49 (CH_2), 31.62 (NCH_3), 31.99 (NCH_3), 45.10 (SCH_3), 45.13 (SCH_3), 45.16 (SCH_3), 47.17 (SCH_3), 162.76 (*C*=N-N), 163.97 (*C*=N-N), 168.26 (N=*C*-S), 169.07 (N=*C*-S) ppm. FAB-MS (MeCN): *m*/*z* 602.4 $[Ru\{Ni(L^2\text{-}Me)\}(dmso)_2]^+$, 524.3 $[Ru\{Ni(L^2\text{-}Me)\}(dmso)]^+$, 446.2 $[Ru\{Ni(L^2\text{-}Me)\}]^+$. *Anal.* Calcd. for $C_{14}H_{30}Cl_2N_6O_2S_4NiRu\cdot(CH_2Cl_2)$: C, 23.81; H, 4.27; N, 11.12%. Found: C, 23.85; H, 4.24; N, 11.22%.

2.4. Preparation of $[RuCl_2\{Ni(L^3\text{-}Et)\}(dmso)_2]$ (**3**)

To a solution of $[RuCl_2(dmso)_4]$ (48.5 mg, 0.10 mmol) in THF (5 mL) was added a solution of $[Ni(L^3\text{-}Et)]$ (37.3 mg, 0.10 mmol) in THF (10 mL), and then the mixture was stirred at reflux overnight, the resulting purple solution was concentrated to ca. 3 mL. Slow addition of diethyl ether gave a purple precipitate, which was filtered, washed by diethyl ether (3 × 5 mL) and hexane (3 × 5 mL), and dried under vacuum. The product was then recrystallized from tetrahydrofuran/diethyl ether to give purple needle-shape crystals. Yield: 60 mg, 70% (based on Ru). IR (KBr disc, cm^{-1}): ν_{NH} 3228 (m); $\nu_{C=N}$ 1621 (m), 1609 (m); $\nu_{S=O}$ 1089 (s); $\nu_{C–S}$ 795 (m). ^1H NMR (400 MHz, DMSO-d_6): δ 7.45 (s, 1H, -N*H*), 6.75 (s, 1H, -N*H*), 3.57 (s, 3H, $-CH_3S$), 3.53 (s, 3H, $-CH_3S$), 3.31 (s, 3H, $-CH_3S$), 3.05 (s, 3H, $-CH_3S$), 2.93 (m, 4H, $-NHCH_2CH_3$), 2.42 (m, 4H, $-CH_2$), 1.98 (s, 3H, $-CH_3$), 1.88 (s, 3H, $-CH_3$), 0.95 (t, *J* = 7.2 Hz, 6H, $-CH_2CH_3$) ppm. ^{13}C NMR (100 MHz, DMSO-d_6): 20.61 (CH_2CH_3), 20.98 (CH_2CH_3), 29.06 (CH_3), 29.18 (CH_3), 31.32 (CH_2), 31.39 (CH_2), 40.71 (NCH_2CH_3), 40.76 (NCH_2CH_3), 43.81 (SCH_3), 43.86 (SCH_3), 43.90 (SCH_3), 45.87 (SCH_3), 162.01 (*C*=N-N), 163.06 (*C*=N-N), 168.83 (N=*C*-S), 169.85 (N=*C*-S) ppm. FAB-MS (MeCN): *m*/*z* 630.5 $[Ru\{Ni(L^3\text{-}Et)\}(dmso)_2]^+$, 552.4 $[Ru\{Ni(L^3\text{-}Et)\}(dmso)]^+$, 474.2 [Ru{Ni($L^3$-Et)}]$^+$. *Anal*. Calcd. for $C_{16}H_{34}Cl_2N_6O_2S_4NiRu$: C, 27.40; H, 4.89; N, 11.98%. Found: C, 27.45; H, 4.85; N, 11.93%.

*2.5. Preparation of [RuCl$_2${Ni(L^4-Ph)}(dmso)$_2$] (**4**)*

To a solution of [RuCl$_2$(dmso)$_4$] (48.5 mg, 0.10 mmol) in DMF (5 mL) was added a solution of [Ni(L^4-Ph)] (46.9 mg, 0.10 mmol) in DMF (10 mL), and then the mixture was stirred at reflux overnight, the resulting black solution was concentrated to ca. 3 mL. Slow addition of diethyl ether gave a black precipitate, which was filtered and washed by diethyl ether (3 × 5 mL) and hexane (3 × 5 mL), and dried under vacuum. Yield: 45 mg, 50% (based on Ru). IR (KBr disc, cm^{-1}): ν_{NH} 3217 (m); $\nu_{C=N}$ 1625 (m), 1603 (m); $\nu_{S=O}$ 1088 (s); $\nu_{C–S}$ 804 (m). ^{1}H NMR (400 MHz, DMSO-d_6): δ 8.28 (s, 1H, -N*H*), 7.83 (s, 1H, -N*H*), 7.23-7.56 (m, 10H, -C_6H_5), 3.60 (s, 3H, -CH_3S), 3.55 (s, 3H, -CH_3S), 3.50 (s, 3H, -CH_3S), 3.46 (s, 3H, -CH_3S), 3.32 (m, 2H, -CH_2), 2.83 (m, 2H, -CH_2), 1.95 (s, 3H, -CH_3), 1.89 (s, 3H, -CH_3) ppm. ^{13}C NMR (100 MHz, DMSO-d_6): 20.52 (CH_3), 20.59 (CH_3), 34.31 (CH_2), 34.36 (CH_2), 36.03 (NCH_3), 36.09 (NCH_3), 43.05 (SCH_3), 43.82 (SCH_3), 45.52 (SCH_3), 45.63 (SCH_3), 119.51(Ar), 123.83 (Ar), 125.24 (Ar), 128.76 (Ar), 134.06 (Ar), 160.86 (*C*=N-N), 161.46 (*C*=N-N), 169.65 (N=*C*-S), 170.06 (N=*C*-S) ppm. FAB-MS (MeCN): *m/z* 726.6 [Ru{Ni(L^4-Ph)}(dmso)$_2$]$^+$, 648.4 [Ru{Ni(L^4-Ph)}(dmso)]$^+$, 570.3 [Ru{Ni(L^4-Ph)}]$^+$. *Anal*. Calcd. for $C_{24}H_{34}Cl_2N_6O_2S_4NiRu$: C, 36.18; H, 4.31; N, 10.56%. Found: C, 36.14; H, 4.27; N, 10.62%.

*2.6. Preparation of [CpRu{Ni(L^1)}(PPh$_3$)]Cl (**5**)*

To a solution of [CpRu(PPh$_3$)$_2$Cl] (72.6 mg, 0.10 mmol) in THF (5 mL) was added a solution of [Ni(L^1)] (31.7 mg, 0.10 mmol) in THF (10 mL), and then the mixture was stirred at room temperature overnight, the resulting dark-green solution was concentrated to ca. 3 mL. Slow addition of diethyl ether gave a dark-green precipitate, which was filtered, washed by diethyl ether (3 × 5 mL) and hexane (3 × 5 mL), and dried under vacuum. Yield: 68 mg, 69% (based on Ru). IR (KBr disc, cm^{-1}): ν_{NH_2} 3436 (m); $\nu_{C=N}$ 1613 (m), 1609 (m); $\nu_{C–P}$ 1091 (m); $\nu_{C–S}$ 791 (m). ^{31}P NMR (162 MHz, DMSO-d_6): δ 54.0 ppm. ^{1}H NMR (400 MHz, DMSO-d_6): δ 7.90 (s, 2H, -NH_2), 6.72 (s, 2H, -NH_2), 7.15-7.43 (m, 15H, -PPh$_3$), 4.32 (s, 5H, -Cp), 2.08 (m, 4H, -CH_2), 2.01 (s, 3H, -CH_3), 1.83 (s, 3H, -CH_3). ^{13}C NMR (100 MHz, DMSO-d_6): 22.24 (CH_3), 22.28 (CH_3), 34.34 (CH_2), 34.39 (CH_2), 77.23 (Cp), 128.42 (Ar), 133.45 (Ar), 137.86 (Ar), 138.83 (Ar), 162.54 (*C*=N-N), 163.14 (*C*=N-N), 169.74 (N=*C*-S), 170.54

(N=*C*-S) ppm. FAB-MS (MeCN): *m/z* 745.0 [CpRu{Ni(L^1}(PPh_3)]$^+$, 483.0 [CpRu{Ni(L^1)}]$^+$. *Anal.* Calcd. for $C_{31}H_{34}ClN_6PS_2NiRu$: C, 47.68; H, 4.39; N, 10.76%. Found: C, 47.62; H, 4.35; N, 10.79%.

*2.7. Preparation of [CpRu{Ni(L^2-Me)}(PPh_3)]Cl·EtOH (**6**·EtOH)*

To a solution of [CpRu(PPh_3)$_2$Cl] (72.6 mg, 0.10 mmol) in THF (5 mL) was added a solution of [Ni(L^2-Me)] (34.5 mg, 0.10 mmol) in THF (10 mL), and then the mixture was stirred at room temperature overnight, the resulting dark green solution was concentrated to ca. 3 mL. Slow addition of diethyl ether gave a green precipitate, which was filtered and washed by diethyl ether (3 × 5 mL) and hexane (3 × 5 mL). The product was then recrystallized from ethanol to give black block-shape crystals. Yield: 75 mg, 73% (based on Ru). IR (KBr disc, cm^{-1}): ν_{NH} 3294 (m); $\nu_{C=N}$ 1603 (m), 1590 (m); ν_{C-P} 1085 (m); ν_{C-S} 802 (m). ^{31}P NMR (162 MHz, DMSO-*d*$_6$): δ 54.0 ppm. ^{1}H NMR (400 MHz, DMSO-*d*$_6$): δ 8.06 (s, 1H, -N*H*), 7.74 (s, 1H, -N*H*), 7.19-7.44 (m, 15H, -P*Ph*$_3$), 4.30 (s, 5H, -Cp), 3.28 (m, 2H, -C*H*$_2$), 2.98 (s, 6H, -NC*H*$_3$), 2.88 (m, 2H, -C*H*$_2$), 2.00 (s, 3H, -C*H*$_3$), 1.81 (s, 3H, -C*H*$_3$). ^{13}C NMR (100 MHz, DMSO-*d*$_6$): 21.03 (*C*H$_3$), 21.09 (*C*H$_3$), 34.23 (*C*H$_2$), 34.28 (*C*H$_2$), 35.76 (N*C*H$_3$), 35.84 (N*C*H$_3$), 77.43 (Cp), 128.55 (Ar), 134.25 (Ar), 138.37 (Ar), 139.53 (Ar), 163.33 (*C*=N-N), 164.23 (*C*=N-N), 170.69 (N=*C*-S), 171.45 (N=*C*-S) ppm. FAB-MS (MeCN): *m/z* 773.1 [CpRu{Ni(L^2-Me)}(PPh_3)]$^+$, 511.0 [CpRu{Ni(L^2-Me)}]$^+$. *Anal.* Calcd. for $C_{33}H_{38}ClN_6PS_2NiRu{\cdot}(C_2H_6O)$: C, 49.18; H, 4.24; N, 11.22%. Found: C, 49.22; H, 4.22; N, 11.25%.

*2.8. Preparation of [CpRu{Ni(L^3-Et)}(PPh_3)]Cl·H_2O (**7**·H_2O)*

To a solution of [CpRu(PPh_3)$_2$Cl] (72.6 mg, 0.10 mmol) in THF (5 mL) was added a solution of [Ni(L^3-Et)] (37.3 mg, 0.10 mmol) in THF (10 mL), and then the mixture was stirred at room temperature overnight, the resulting dark green solution was concentrated to ca. 3 mL. Slow addition of diethyl ether gave a green precipitate, which was filtered and washed by diethyl ether (3 × 5 mL) and hexane (3 × 5 mL). The product was then recrystallized from ethanol to give black block-shape crystals. Yield: 64 mg, 70% (based on Ru). IR (KBr disc, cm^{-1}): ν_{NH} 3286 (m); $\nu_{C=N}$ 1604 (w), 1596 (m); ν_{C-P} 1086 (m); ν_{C-S} 802 (m). ^{31}P NMR (162 MHz, DMSO-*d*$_6$): δ 54.4 ppm. ^{1}H NMR (400 MHz, DMSO-*d*$_6$): δ 7.96 (s, 1H, -N*H*), 7.70 (s, 1H, -N*H*), 7.10-7.45 (m, 15H, -P*Ph*$_3$), 4.31 (s, 5H, -Cp), 3.40 (m, 2H, -C*H*$_2$), 3.06 (m, 4H, -C*H*$_2$NH), 2.88 (m, 2H, -C*H*$_2$), 1.99 (s, 3H, -C*H*$_3$), 1.91 (s, 3H, -C*H*$_3$), 0.94 (t, *J* = 7.2 Hz, 6H, -CH$_2$C*H*$_3$). ^{13}C NMR (100 MHz, DMSO-*d*$_6$): 15.56 (NCH$_2$*C*H$_3$), 15.62 (NCH$_2$*C*H$_3$), 29.01

(CH_3), 29.07 (CH_3), 34.18 (CH_2), 34.23 (CH_2), 41.06 (NCH_2CH_3), 41.12 (NCH_2CH_3), 77.64 (Cp), 128.75 (Ar), 134.05 (Ar), 137.95 (Ar), 139.27 (Ar), 161.12 (*C*=N-N), 161.23 (*C*=N-N), 170.15 (N=*C*-S), 171.00 (N=*C*-S) ppm. FAB-MS (MeCN): *m*/*z* 801.1 [CpRu{Ni(L^3-Et)(PPh_3)]$^+$, 539.0 [CpRu{Ni(L^3-Et)}]$^+$. *Anal*. Calcd. for $C_{35}H_{42}ClN_6PS_2NiRu$: C, 50.23; H, 5.06; N, 10.05%. Found: C, 50.19; H, 5.03; N, 10.09%.

*2.9. Preparation of [CpRu{Ni(L^4-Ph)}(PPh_3)]Cl (**8**)*

To a solution of [CpRu(PPh_3)$_2$Cl] (72.6 mg, 0.10 mmol) in THF(5 mL) was added a solution of [Ni(L^4-Ph)] (46.9 mg, 0.10 mmol) in THF (10 mL), and then the mixture was stirred at room temperature overnight, the resulting dark-green solution was concentrated to ca. 3 mL. Slow addition of diethyl ether gave a dark-green precipitate, which was filtered, washed by diethyl ether (3 × 5 mL) and hexane (3 × 5 mL), and dried under vacuum. Yield: 73 mg, 61% (based on Ru). IR (KBr disc, cm^{-1}): ν_{NH} 3233 (m); $\nu_{C=N}$ 1621 (m), 1611 (m); $\nu_{C\text{–}P}$ 1082 (m); $\nu_{C\text{–}S}$ 798 (m). ^{31}P NMR (162 MHz, DMSO-d_6): δ 54.7 ppm. ^{1}H NMR (400 MHz, DMSO-d_6): δ 8.00 (s, 1H, -N*H*), 7.72 (s, 1H, -N*H*), 7.10-7.46 (m, 15H, -PPh_3, -C_6H_5), 4.35 (s, 5H, -Cp), 3.32 (m, 2H, -CH_2), 2.81 (m, 2H, -CH_2), 1.90 (s, 3H, -CH_3), 1.81 (s, 3H, -CH_3). ^{13}C NMR (100 MHz, DMSO-d_6): 22.71 (CH_3), 22.716 (CH_3), 33.68 (CH_2), 33.75 (CH_2), 76.94 (Cp), 119.53 (Ar), 123.84 (Ar), 128.75 (Ar), 134.05 (Ar), 137.94 (Ar), 138.04 (Ar), 139.24 (Ar), 163.86 (*C*=N-N), 164.56 (*C*=N-N), 172.42 (N=*C*-S), 173.12 (N=*C*-S) ppm. FAB-MS (MeCN): *m*/*z* 897.1 [CpRu{Ni(L^4-Ph)}(PPh_3)]$^+$, 635.0 [CpRu{Ni(L^4-Ph)}]$^+$. *Anal*. Calcd. for $C_{43}H_{42}ClN_6PS_2NiRu$: C, 55.36; H, 4.54; N, 9.01%. Found: C, 55.32; H, 4.51; N, 9.05%.

2.10. X-Ray crystallography

A summary of crystallographic data and experimental details for complexes **2**·CH_2Cl_2, **6**·EtOH, and **7**·H_2O are listed in Table 1. Intensity data were collected on a Bruker SMART APEX 2000 CCD diffractometer using graphite-monochromated Mo-Kα radiation (λ = 0.71073 Å) at 293(2) K. The data was corrected for absorption using the program SADABS [24]. Structures were solved by the direct methods and refined by full-matrix least-squares on F^2 using the SHELXTL software package [25, 26]. All non-hydrogen atoms were refined anisotropically. Hydrogen atoms in the phenyl and other organic moieties were treated as idealized contributions (C_{sp3}–H = 0.96, C_{sp2}–H = 0.93 Å, and N–H =

0.86–0.93 Å). The ethanol solvent molecule in **6**·EtOH and water molecule in **7**·H_2O was refined without hydrogen atoms.

2.11. Typical procedure for acetalation of benzaldehyde with ethanol in the presence of NiRu complexes and H_2

The catalyst solution was prepared by dissolving complex **2** (0.005 mmol) in acetonitrile (60 mL). Under 1 atm hydrogen atmosphere, a mixture of aldehyde (2.0 mmol), 6 mL of the catalyst solution (0.0005 mmol), and ethanol (12 mL) was stirred at room temperature for four hours. After the reaction was complete, the reaction mixture was concentrated under reduced pressure and subjected to elimination of catalyst by silica gel column chromatography using ethyl acetate/n-hexane (v:v = 1:5) mixed solvents as eluent to afford the product, which was identified through GC-MS analysis.

3. Results and discussion

Treatment of the metalloligands [Ni(L-R)] with *cis*-$[RuCl_2(dmso)_4]$ in DMF or THF at reflux afforded neutral "Ni(μ-S)$_2$Ru" bimetallic complexes of the type $[RuCl_2\{Ni(L\text{-}R)\}(dmso)_2]$ (**1**–**4**), two dmso ligands in *cis*-$[RuCl_2(dmso)_4]$ were replaced by the [Ni(L-R)] units. Reactions of $[CpRu(PPh_3)_2Cl]$ and the metalloligands [Ni(L-R)] in THF at room temperature led to isolation of the expected cationic "Ni(μ-S)$_2$Ru" complexes $[CpRu\{Ni(L\text{-}R)\}(PPh_3)]Cl$ (**5**–**8**) in moderate to good yields. One triphenylphosphine and one chloro ligands in $[CpRu(PPh_3)_2Cl]$ were substituted by the [Ni(L-R)] units and the left chloro ligand acted as the counter anion in the formation of complexes **5–8** (Scheme 1), which may be monitored by *in situ* ^{31}P NMR spectroscopy, showing known signals of the free PPh_3 (δ = –6.65 ppm) and the oxidized $OPPh_3$ (δ = 22.8 ppm) along with a new signal (δ = 54.0 ppm) of the final product. Complexes **1–4** are air-stable in the solid state but easily oxygenates when exposed to air in solution for a couple of hours, whereas complexes **5–8** are relatively air-stable both in solution and in the solid state, possibly due to the presence of strong σ-donor triphenylphosphine ligand.

The IR spectra of complexes **1**–**8** clearly show two intense bands of $\nu_{C=N}$ at around 1600 and 1590 cm^{-1}, one medium band of ν_{N-H} in the region 3500–3200 cm^{-1}, and the band at about 800 cm^{-1} due to the ν_{C-S} mode, indicating the thiol form of L-R ligands (Chart 2) [19, 27, 28]. The presence of PPh_3 in complexes **5–8** is confirmed by the observation of a characteristic ν_{P-C} band in the range 1082–

1091 cm^{-1}. In addition, the $\nu_{S=O}$ band, observed at approximately 1090 cm^{-1} in complexes **1–4**, confirms the presence of sulfur-bonded dmso in the ruthenium coordination sphere [29]. The ^{1}H NMR spectra of complexes **1**–**4** all show a singlet for the CH_3S group protons at around 3.5 ppm. The Cp group in complexes **5–8** exhibited as a singlet at about 4.3 ppm, which is compared with that in related ruthenium complexes [30]. The ^{31}P NMR spectra of complexes **5**–**8** displayed PPh$_3$ signals at around 54.0 ppm, similar to that in the related complex [CpRu(PPh$_3$)S$_2$CNSi^{i}Pr$_3$(1-Naphth)] (53.7 ppm) [30]. The ^{13}C NMR spectra of complexes **1**–**8** showed peaks at around 170 and 165 ppm for the N=*C*–S and *C*=N–N moieties, respectively. The positive ion FAB mass spectra of **1**–**8** showed the expected peaks which corresponded to the cation ions [Ru{Ni(L-R)}(dmso)$_2$]$^+$ or [CpRu{Ni(L-R)}(PPh$_3$)]$^+$, and [Ru{Ni(L-R)}(dmso)]$^+$ or [CpRu{Ni(L-R)}]$^+$ with the characteristic isotopic distribution patterns.

The molecular structures of complexes **2**·CH$_2$Cl$_2$, **6**·EtOH, and **7**·H$_2$O have been established by single-crystal X-ray crystallography. Complex **2**·CH$_2$Cl$_2$ crystallizes in monoclinic $P2_1/c$ space group, while complexes **6**·EtOH and **7**·H$_2$O both crystallize in monoclinic $P2_1/n$ space group. The structures of [RuCl$_2${Ni(L^2-Me)}(dmso)$_2$] in **2**·CH$_2$Cl$_2$ and cationic parts [CpRu{Ni(L-R)}(PPh$_3$)] in **6**·EtOH and **7**·H$_2$O are depicted in Figs. 1–3, respectively. Selected bond lengths and bond angles for complexes **2**·CH$_2$Cl$_2$, **6**·EtOH, and **7**·H$_2$O and some related complexes are summarized in Table 2 for comparison. The C–S bond lengths ranging from 1.781(3) to 1.798(3) Å, together with the (S)C=N bond lengths ranging from 1.285(4) to 1.307(4) Å for thiosemicarbazonato fragments in complexes **2**·CH$_2$Cl$_2$, **6**·EtOH, and **7**·H$_2$O, further imply their binegative thiol form of L-R ligands [17, 18, 31]. The structures of {Ni(L-R)} unit in complexes **2**·CH$_2$Cl$_2$, **6**·EtOH, and **7**·H$_2$O all have 5:7:5-membered chelate ring systems. The coordination around the nickel atoms involve a distortion from the square planarity and the ruthenium atoms all adopt a distorted-octahedral coordination in complexes **2**·CH$_2$Cl$_2$, **6**·EtOH, and **7**·H$_2$O. For complex **2**·CH$_2$Cl$_2$, the ruthenium atom is surrounded by two sulfur atoms from the metalloligand [Ni(L^2-Me)], two *cis* chloro and two sulfur atoms from two *cis* S-bonded dmso ligands. For complexes **6**·EtOH and **7**·H$_2$O, the ruthenium atoms are surrounded by one Cp ring, one triphenylphosphine ligand and the metalloligand [Ni(L-R)]. The Ru–S$_{dmso}$ bond lengths of 2.2485(8) and 2.2679(8) Å, Ru–Cl bond lengths of 2.4201(9) and 2.4459(9) Å, as well as the Cl–Ru–Cl bond angle of 89.19(3)^o in complex **2**·CH$_2$Cl$_2$, agree well with those in other similar complex [RuCl$_2$(dmso)$_2$(MeS(CH$_2$)$_2$SMe)] (2.2676(8), 2.3104(9) Å; 2.4193(9), 2.4438(9) Å; 89.81(4)^o) [32]. The average Ru–C bond length is 2.179(3) Å in complex **7**·H$_2$O, similar to that of 2.179(2) Å in complex **6**·EtOH.

Complexes **2**·CH_2Cl_2, **6**·EtOH, and **7**·H_2O all contain a NiS_2Ru butterfly core, in which the nickel and ruthenium atoms are located in wing, joined by a pair of bidentate thiolato ligands as the body of the butterfly. The dihedral angles of two NiS_2 and RuS_2 trianglar planes are 50.24(4)^o for complex **2**·CH_2Cl_2, 50.13(3)^o for complex **6**·EtOH, and 49.01(2)^o for complex **7**·H_2O, which are much smaller than that of 74.35(6)^o in complex $[CpRu\{Ni(tsalphen)\}(PPh_3)]^+$ (tsalphen = *N*,*N*'-bis(2-thiobenzylidene)-1,2-phenylenediaminato) [21], suggesting the $\{NiN_2S_2\}$ unit is obviously crucial for the butterfly structure. The Ni···Ru distances in complexes **2**·CH_2Cl_2, **6**·EtOH, and **7**·H_2O are similar, being 3.173 Å for complex **2**·CH_2Cl_2, 3.116 Å for complex **6**·EtOH, and 3.139 Å for complex **7**·H_2O, which lie in the range of 2.877–3.352 Å in other reported bimetallic [Ni(μ-S)Ru] complexes [20, 33, 34], though obviously longer than that in the hydrido-bridged $Ni(\mu\text{-}H)(\mu\text{-}S)_2Ru$ complex $[(Ni^{II}L)(H_2O)(\mu\text{-}H)Ru^{II}(\eta^6\text{-}C_6Me_6)](NO_3)$ (L = *N*,*N′*-dimethyl-*N*,*N′*-bis(2-mercaptoethyl)-1,3-propanediamine) (2.739(3) Å) [8]. The bond angle of N(2)–Ni(1)–S(1) (168.10(8)°) is almost the same to N(1)–Ni(1)–S(2) (168.38(8)°) in the somewhat symmetrical complex **2**·CH_2Cl_2. However, in cationic complexes **6**·EtOH and **7**·H_2O, the N(2)–Ni(1)–S(1) bond angles (173.05(8)° for **6**·EtOH and 172.64(6)° for **7**·H_2O) are obviously larger than those of N(1)–Ni(1)–S(2) bond angles (164.79(8)^o for **6**·EtOH and 165.07(6)^o for **7**·H_2O). The Ni–S–Ru angles of 87.15(3) and 87.98(3)°in **2**·CH_2Cl_2 are a little larger than those of 84.22(3) and 85.95(3)° in **6**·EtOH, as well as 84.97(2) and 86.65(2)° in **7**·H_2O, a suggestive of the ruthenium surroundings also having influence on the core structure of $\{Ni(\mu\text{-}S)_2Ru\}$. The S–Ru–S bond angle of 77.83(3)° in **6**·EtOH is similar to that in **7**·H_2O (77.48(2)°), indicating the alkyl substituent on thiosemicarbazonato ligands have little effect on the bond parameters.

As stated above, Ogo and coworkers have reported that complex $[(Ni^{II}L)(H_2O)Ru^{II}(\eta^6\text{-}C_6Me_6)]^{2+}$ could catalyze the heterolytic cleavage of hydrogen molecules and followed isolation of a hydrido bridged species $[(Ni^{II}L)(H_2O)(\mu\text{-}H)Ru^{II}(\eta^6\text{-}C_6Me_6)]^+$ [8]. Moreover, complex $[(\eta^6\text{-}p\text{-}cymene)Ru\{Ni(tsalphen)\}(MeCN)](OTf)_2$ was found to catalyze acetalation of benzaldehyde with ethanol in the presence of H_2 [21]. Complex **2** was thus tested in such reactions and benzaldehyde diethyl acetal $[C_6H_5CH(OCH_2CH_3)_2]$ was also observed from GC-MS analysis (Fig. 4), suggesting that acetalation of benzaldehyde took place in the presence of complex **2** and H_2. Controlled reaction without participation of H_2 did not give the acetal product, presenting H_2 being the source of H^+, a prerequisite for the acetalation reaction. The pH measurements were performed on the reaction process, which showed that the pH of the solution decreased (from pH 6.4 to pH 5.1), indicating the heterolytic

H_2 cleavage [8, 35]. Based on Ogo's work [8], the possible mechanism of the acetalization of PhCHO is proposed as following: (1) One of the labile dmso ligands on ruthenium center in complex **2** left and a coordinately unsaturated species {$RuCl_2$\{Ni(L^2-Me)}(dmso)} formed. (2) Heterocleavage of H_2 produced the hydrido-bridged species {$RuCl_2$\{Ni(L^2-Me)}(dmso)(μ-H)} along with the active protons. (3) The resulted protons catalyzed the typical acetalation of benzaldehyde and ehanol. The effect of temperature, reaction time and the amount of catalyst on acetalation reaction were investigated in detail (see Table 3). When the temperature increased from 0 ^{o}C to 60 ^{o}C, the conversion of benzaldehyde increased from 2.4% to 15.5%, suggesting that the relatively higher temperature benefits the reaction. Although the higher temperatures did not lead to obvious increase after 40 ^{o}C, as a matter of the fact, the reactions might be done at 40 ^{o}C for the following attempts. Longer reaction time also led to a little increase of conversion (entries 5 to 10). As expected, the conversion increased with the increased amount of bimetallic {Ni(μ-S)$_2$Ru} complex **2** (entries 11 and 12). The substituent of methyl, ethyl, or phenyl seemed to have little effect on the catalytic activity (entries 11 and 13–15). When complexes **5**–**8** were used to initiate the reaction, the compound benzaldehyde diethyl acetal was also observed. Therefore, the conversions in this catalytic system may be compared with that in other transition metal catalyzed ethanolysis of benzaldehyde [36].

In summary, although bis(thiosemicarbazonato)nickel(II) complexes with tetradentate tricyclic-ligand systems were reported as early as 1970 by McCleverty [31], these mononuclear nickel(II) complexes have not been employed to further construct heterobimetallic complexes according to a CCDC search. Syntheses and characterization of a series of thiolate-bridged bimetallic nickel-ruthenium complexes based on hexane-2,5-dione bis(thiosemicarbazonato)-nickel(II) units were reported in this paper. X-Ray diffraction studies may establish the thiol form of thiosemicarbazonato moieties due to the characteristic C–S bond lengths ranging from 1.781(3) to 1.797(2) Å in complexes **2**·CH_2Cl_2, **6**·EtOH, and **7**·H_2O. The Ni···Ru distances in complexes **2**·CH_2Cl_2, **6**·EtOH, and **7**·H_2O are 3.173, 3.116, and 3.139 Å, respectively, which agree well with those in other related bimetallic nickel-ruthenium complexes with [NiN_2S_2] metalloligands [20, 21, 33, 34]. The triphenylphosphine ligands may stabilize the {Ni(μ-S)$_2$Ru} complexes **6**·EtOH and **7**·H_2O, indicated by their slightly shorter Ni···Ru distances. Complexes **1**–**8** could effectively catalyze acetalation of benzaldehyde with ethanol in the presence of 1 atm molecular H_2.

4. Supplementary material

Crystallographic data for [$RuCl_2$\{Ni(L^2-Me)\}($(dmso)_2$)]·CH_2Cl_2 (**2**), [CpRu\{Ni(L^2-Me)\}(PPh_3)]Cl·EtOH (**6**), and [CpRu\{Ni(L^3-Et)\}(PPh_3)]Cl·H_2O (**7**·H_2O) have been deposited with the Cambridge Crystallographic Data Centre as supplementary publication nos. CCDC 1840252, 1840253, and 1840254, respectively. Copies of the data can be obtained free of charge on application to CCDC, 12 Union Road, Cambridge CB2 1EZ, UK [fax: (+44)1233-336-033; e-mail: deposit@ccdc.cam.ac.uk].

Acknowledgements

This project was supported by the Natural Science Foundation of China (grant no. 21372007). We thank the reviewers' helpful suggestion during the revision of this paper.

References

[1] W. Lubitz, H. Ogata, O. Rüdiger, E. Reijerse, Hydrogenases. Chem. Rev. 114 (2014) 4081-4148.

[2] A. Volbeda, M.-H. Charon, C. Piras, E. C. Hatchikian, M. Frey, J.C. Fontecilla-Camps, Crystal structure of the nickel–iron hydrogenase from Desulfovibrio gigas. Nature 373 (1995) 580-587.

[3] H. Ogata, K. Nishikawa, W. Lubitz, Hydrogens detected by subatomic resolution protein crystallography in a [NiFe] hydrogenase. Nature 520 (2015) 571-574.

[4] Y. Shomura, M. Taketa, H. Nakashima, H. Tai, H. Nakagawa, Y. Ikeda, M. Ishii, Y. Igarashi, H. Nishihara, K.-S. Yoon, S. Ogo, S. Hirota, Y. Higuchi, Structural basis of the redox switches in the NAD+-reducing soluble [NiFe]-hydrogenase. Science 357 (2017) 928-932.

[5] B.E. Barton, T.B. Rauchfuss, Hydride-containing models for the active site of the nickel–iron hydrogenases. J. Am. Chem. Soc. 132 (2010) 14877-14885.

[6] D. Brazzolotto, M. Gennari, N. Queyriaux, T. R. Simmons, J. Pécaut, S. Demeshko, F. Meyer, M. Orio, V. Artero, C. Duboc, Nickel-centred proton reduction catalysis in a model of [NiFe] hydrogenase. Nat. Chem. 8 (2016) 1054-1060.

[7] L.-C. Song, Y. Lu, L. Zhu, Q.-L Li,. Dithiolato- and diselenolato-bridged nickel-iron biomimetics for the active site of [NiFe]hydrogenases. Organometallics 36 (2017) 750-760.

[8] S. Ogo, R. Kabe, K. Uehara, B. Kure, T. Nishimura, S.C. Menon, R. Harada, S. Fukuzumi, Y. Higuchi, T. Ohhara, T. Tamada, R. Kuroki, A dinuclear Ni(μ-H)Ru complex derived from H_2. Science 316 (2007) 585-587.

[9] S. Canaguier, V. Fourmond, C.U. Perotto, J. Fize, J. Pécaut, M. Fontecave, M.J. Field, V. Artero, Catalytic hydrogen production by a Ni–Ru mimic of NiFe hydrogenases involves a proton-coupled electron transfer step. Chem. Commun. 49 (2013) 5004-5006.

[10] G.M. Chambers, J. Mitra, T.B. Rauchfuss, M. Stein, Ni^I/Ru^{II} model for the Ni-L state of the [NiFe]hydrogenases: Synthesis, spectroscopy, and reactivity. Inorg. Chem. 53 (2014) 4243-4249.

[11] S. Ogo, H_2 and O_2 activation by [NiFe]hydrogenases – Insights from model complexes. Coord. Chem. Rev. 334 (2017) 334, 43-53.

[12] J.S. Casas, M.S. García-Tasende, J. Sordo, Main group metal complexes of semicarbazones and thiosemicarbazones. A structural review. Coord. Chem. Rev. 209 (2000) 197-261.

[13] J.R. Dilworth, R. Hueting, Metal complexes of thiosemicarbazones for imaging and therapy. Inorg. Chim. Acta 389 (2012) 3-15.

[14] K. Alomar, A. Landreau, M. Allain, G. Bouet, G. Larcher, Synthesis, structure and antifungal activity of thiophene-2,3-dicarboxaldehyde bis(thiosemicarbazone) and nickel(II), copper(II) and cadmium(II) complexes: Unsymmetrical coordination mode of nickel complex. J. Inorg. Biochem. 126 (2013) 76-83.

[15] A.P. King, H.A. Gellineau, J.-E. Ahn, S.N. MacMillan, J.J. Wilson, Bis(thiosemicarbazone) complexes of cobalt(III). Synthesis, characterization, and anticancer potential. Inorg. Chem. 56 (2017) 6609-6623.

[16] J.K. Bilyj, M.J. Riley, P.V. Bernhardt, Isomerism and reactivity of nickel(II) acetylacetonate bis(thiosemicarbazone) complexes. Dalton Trans. 47 (2018) 2018-2030.

[17] A.K. Nandi, S. Chaudhuri, S.K. Mazumdar, Crystal and molecular structure of hexan-2,5dione bis(4-phenyl-thiosemicarbazonato)nickel(II), ($C_{20}H_{22}N_6S_2Ni$): A model study of the enhancement of the antibacterial activity of a tetradentate N, S donor ligand on metal complexation. Inorg. Chim. Acta 92 (1984) 235-240.

[18] M.S. Shalamzari, A.V. Gurbanov, S. Heidic, R. Kia, S. Behrouzi, [Hexane-2,5-dione bis(thiosemicarbazonato)]nickel(II). Acta Crystallogr. E69 (2013) m322-328.

[19] B.Jeragh, A.A. El-Asmy, Coordination of Fe(III), Co(II), Ni(II), Cu(II), Zn(II), Cd(II), Hg(II), Pd(II) and Pt(II) with 2,5-hexanedione bis(thiosemicarbazone), L: Crystal structure of *cis*-$[Pd(L)]Cl_2$ and 1-(2,5-dimethyl-1H-pyrrol-yl)-thiourea. Spectrochim. Acta A 130 (2014) 546-552.

[20] M.A. Reynolds, T.B. Rauchfuss, S.R. Wilson, Ruthenium derivatives of NiS_2N_2 complexes as analogues of bioorganometallic reaction centers. Organometallics 22 (2003) 1619-1625.

[21] A.-Q. Jia, L.-H. Tang, X.-P. Dong, Z. Xin, Q.-F. Zhang, Syntheses, structures and reactivity of dinuclear organorutheniumnickel complexes with *N,N′*-bis(2-thiobenzylidene)-1,2-phenylenediaminato (tsalphen) ligand. J. Organomet. Chem. 858 (2018) 23-28.

[22] I. Bratsos, E. Alessio, Inorg. Synth. 35 (2010) 148-152.

[23] M.I. Bruce, C. Hameister, A.G. Swincer, R.C. Wallis, Inorg. Synth. 21 (1982) 78-79.

[24] G.M. Sheldrick, *SADABS*; University of Göttingen: Germany, 1996.

[25] G.M. Sheldrick, *SHELXTL Software Reference Manual (Version 5.1)*, Bruker AXS Inc., Madison, WI, 1997.

[26] G.M. Sheldrick, A short history of SHELXTL. Acta Crystallogr. A64 (2008) 112-122.

[27] P.K.Suganthy, R.N. Prabhu,, V.S. Sridevi, Nickel(II) thiosemicarbazone complex catalyzed Mizoroki–Heck reaction. Tetrahrdron Lett. 54 (2013) 5695-5698.

[28] T.S. Lobana, G. Bawa, R.J. Butcher, Synthesis of Cu^{II}-Ru^{II}-Cu^{II} trinuclear complexes via redox reaction of copper(I) across thiosemicarbazones coordinated to ruthenium(II). Inorg. Chem. 47 (2008) 1488-1495.

[29] L. Otero, P. Noblia, D. Gambino, H. Cerecetto, M. González, J.A. Ellena, O.E. Piro, Inorg. Chim. Acta 344 (2003) 85-94.

[30] I. Kovács, A.-M. Lebuis, A. Shaver, Ruthenium-assisted insertion of isothiocyanates into the silicon-sulfur bond: A comparative study on the reactivity of the S-Si and S-H bonds in $CpRu(PPh_3)_2SX$ (X = H, Si^iPr_3) complexes. Organometallics 20 (2001) 35-41.

[31] N.A. Bailey, S.E. Hull, C.J. Jones, J.A. McCleverty, The electrochemical properties and crystal structures of Some nickel diketone bisthiosernicarbazones. Chem. Commun. (1970) 124-126.

[32] S. Olsson, P.M. Bjçremark, T. Kokoli, J. Sundberg, A. Lennartson, C.J. McKenzie, M. Håkansson, Absolute asymmetric synthesis: Protected substrate oxidation. Chem. Eur. J. 21 (2015) 5211-5219.

[33] T. Matsumoto, K. Yoshimoto, C. Zheng, Y. Shomura, Y. Higuchi, H. Nakai, S. Ogo, Synthesis and reactivity of a water-soluble NiRu monohydride complex with a tethered pyridine moiety. Chem. Lett. 45 (2016) 197-199.

[34] K. Kim, T. Kishima, T. Matsumoto, H. Nakai, S. Ogo, Selective redox activation of H_2 or O_2 in a [NiRu] complex by aromatic ligand effects. Organometallics 32 (2013) 79-87.

[35] A.C. Ontko, J.F. Houlis, R.C. Schnabel, D.M. Roddick, T.P. Fong, A.J. Lough, R.H. Morris, Protonation and H_2 heterolysis reactions of electrophilic (η^5-C_5R_5)Ru(dfepe)(X) (R = H, Me; X = H, OTf) complexes. Organometallics 17 (1998) 5467-5476.

[36] U.S.F. Arrozi, H.W. Wijaya, A. Patah, Y. Permana, Efficient acetalization of benzaldehydes using UiO-66 and UiO-67: Substrates accessibility or Lewis acidity of zirconium. Appl. Catal. A: Gen. 506 (2015) 77-84.

Table 1.

Crystallographic data and experimental details for $[RuCl_2\{Ni(L\text{-}Me)\}(dmso)_2]\cdot CH_2Cl_2$ (**2**$\cdot CH_2Cl_2$), $[CpRu\{Ni(L\text{-}Me)\}(PPh_3)]Cl\cdot EtOH$ (**6**·EtOH), and $[CpRu\{Ni(L\text{-}Et)\}(PPh_3)]Cl$ (**7**$\cdot H_2O$).

complex	**2**$\cdot CH_2Cl_2$	**6**·EtOH	**7**$\cdot H_2O$
empirical formula	$C_{15}H_{32}Cl_4N_6O_2S_4NiRu$	$C_{35}H_{38}ClN_6OPS_2NiRu$	$C_{35}H_{44}ClN_6OPS_2NiRu$
formula weight	758.28	849.03	855.08
crystal system	monoclinic	monoclinic	monoclinic
a (Å)	10.710(3)	13.7443(11)	13.972(2)
b (Å)	32.865(8)	19.4666(16)	19.742(2)
c (Å)	8.2559(19)	14.0206(11)	14.218(2)
α(°)	90	90	90
β (°)	102.711(3)	95.9420(10)	97.456(1)
γ(°)	90	90	90
V (Å^3)	2834.8(11)	3731.1(5)	3888.9(8)
space group	$P2_1/c$	$P2_1/n$	$P2_1/n$
Z	4	4	4
D_{calc} (g cm^{-3})	1.777	1.511	1.460
temperature (K)	296(2)	296(2)	296(2)
F(000)	1536	1736	1760
μ(Mo-Kα) (mm^{-1})	1.894	1.173	1.125
total refln	17401	22988	23910
independent refln	6502	8532	8951
parameters	314	427	437
R_{int}	0.0284	0.0350	0.0208
$R1^a$, $wR2^b$ ($I > 2\sigma(I)$)	0.0339, 0.0717	0.0341, 0.0908	0.0286, 0.0754
$R1$, $wR2$ (all data)	0.0430, 0.0760	0.0521, 0.1075	0.0379, 0.0819
GoF^c	1.017	0.820	0.950

[a] $R1 = ||F_o| - |F_c||/|F_o|$.

[b] $wR2 = [w(|F_o^2| - |F_c^2|)^2/w|F_o^2|^2]^{1/2}$.

[c] $GoF = [w(|F_o| - |F_c|)^2/(N_{obs} - N_{param})]^{1/2}$.

Table 2.

Comparison of selected bond lengths (Å) and angles (deg) for complexes **2**·CH_2Cl_2, **6**·EtOH and **7**·H_2O, and some related nickel complexes.

	2·CH_2Cl_2	**6**·EtOH	**7**·H_2O	**Ni(L-H)**	**Ni(L-Ph)**
C–S	1.792(3)	1.791(3)	1.789(2)	1.7434(14)	1.721(5)
	1.781(3)	1.798(3)	1.797(2)	1.7374(15)	1.776(4)
(S)C=N	1.285(4)	1.288(4)	1.294(3)	1.3051(17)	1.290(5)
	1.287(4)	1.307(4)	1.303(3)	1.2887(18)	1.293(6)
C–NHR	1.341(4)	1.333(4)	1.331(3)	1.3392(19)	1.357(5)
	1.344(4)	1.343(4)	1.341(3)	1.3619(18)	1.368(1)
(Me)C=N	1.282(4)	1.301(4)	1.294(3)	1.2816(18)	1.296(5)
	1.293(4)	1.286(4)	1.284(3)	1.2923(17)	1.294(6)
N–N	1.412(4)	1.418(4)	1.414(3)	1.4202(17)	1.413(5)
	1.425(4)	1.411(3)	1.413(3)	1.4181(15)	1.429(5)
Ni–S	2.1657(9)	2.1801(8)	2.1813(6)	2.1542(4)	2.147(1)
	2.1642(10)	2.1656(8)	2.1632(6)	2.1718(4)	2.163(1)
Ni–N	1.913(2)	1.952(2)	1.9554(19)	1.9155(11)	1.903(3)
	1.960(3)	1.896(2)	1.9008(18)	1.9751(12)	1.937(4)
Ru–S(1)	2.4285(8)	2.4570(8)	2.4570(6)	-	-
Ru–S(2)	2.3973(9)	2.3990(7)	2.4047(6)	-	-
S–Ni–S	85.62(3)	89.17(3)	88.91(2)	88.755(14)	87.8(1)
N–Ni–N	102.08(11)	99.46(10)	99.81(8)	101.11(5)	130.4(4)
S–Ru–S	75.14(3)	77.83(3)	77.48(2)	-	-
Ru···Ni	3.173	3.116	3.139	-	-

Table 3.
Acetalization[a] of benzaldehyde with ethanol in the presence of Ni-Ru complexes and H_2.

entry	catalyst	temperature/°C	time/h	conversion/%
1	**2**	0	4	2.4
2	**2**	15	4	7.8
3	**2**	40	4	13.2
4	**2**	60	4	15.5
5	**2**	40	1	4.4
6	**2**	40	2	8.5
7	**2**	40	3	10.3
8	**2**	40	4	13.2
9	**2**	40	5	15.2
10	**2**	40	10	16.3
11	**2**[b]	40	4	33.7
12	**2**[c]	40	4	37.0
13	**1**[b]	40	4	32.0
14	**3**[b]	40	4	33.6
15	**4**[b]	40	4	33.1
16	**5**[b]	40	4	24.2
17	**6**[b]	40	4	25.6
18	**7**[b]	40	4	26.0
19	**8**[b]	40	4	25.3

[a] Reactions were monitored by TLC/GC.

[b] The amount of catalyst is 0.001 mmol (twice of that in entry 3).

[c] The amount of catalyst is 0.025 mmol (five times of that in entry 3).

Chart 1. The structures of four kinds of [NiN_2S_2] metalloligands in NiRu complexes.

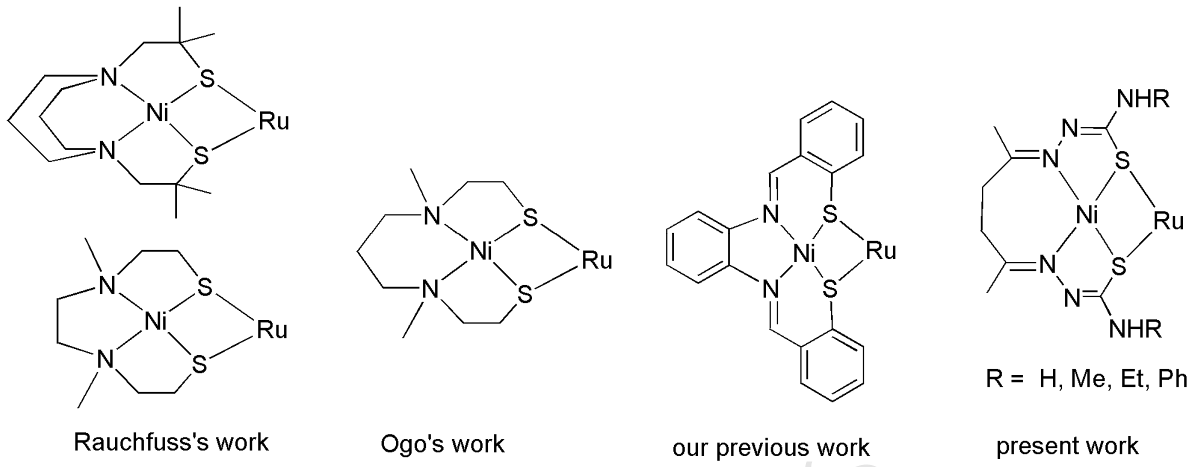

Rauchfuss's work

Ogo's work

our previous work

present work

Chart 2. The thione and thiolene forms of hexane-2,5-dione bis(thiosemicarbazones).

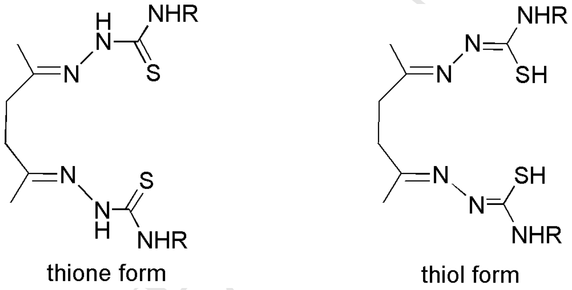

thione form

thiol form

Scheme 1. Synthesis of heterobimetallic ruthenium-nickel complexes **1–8**.

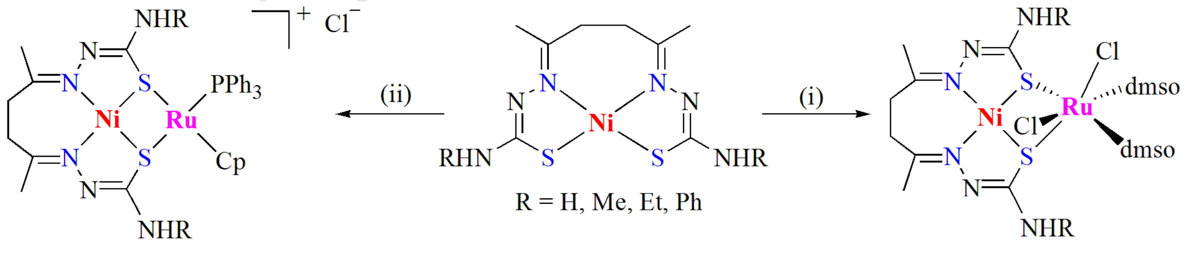

5, R = H; **6**, R = Me
7, R = Et; **8**, R = Ph

1, R = H; **2**, R = Me
3, R = Et; **4**, R = Ph

(i) $Ru(dmso)_4Cl_2$; (ii) $CpRuCl(PPh_3)_2$

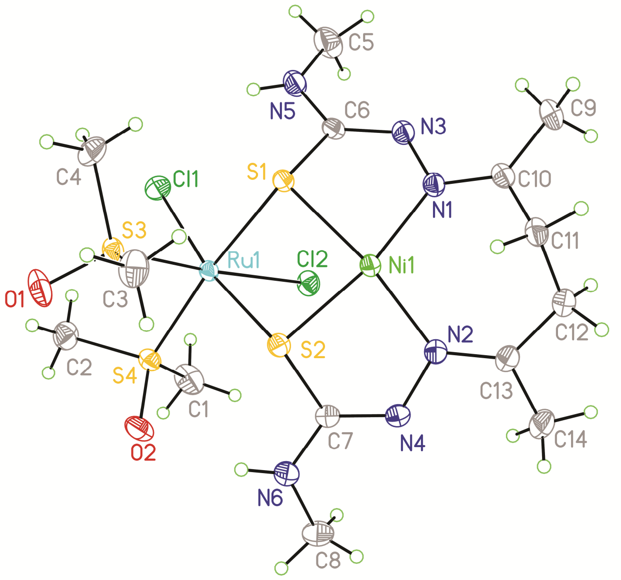

Fig. 1. Molecular structure of the cation of [RuCl$_2${Ni(L^2-Me)}(dmso)$_2$]·CH$_2$Cl$_2$ (**2**·CH$_2$Cl$_2$), with thermal ellipsoids drawn at the 40% probability level. Solvent molecule is omitted for clarity. Selected bonds (Å) and angles (°): Ru(1)–S(1) 2.4285(8), Ru(1)–S(2) 2.3973(9), Ru(1)–S(3) 2.2485(8), Ru(1)–S(4) 2.2679(8), Ru(1)–Cl(1) 2.4201(9), Ru(1)–Cl(2) 2.4459(9), Ru(1)···Ni(1) 3.173, Ni(1)–N(1) 1.913(2), Ni(1)–N(2) 1.960(3), Ni(1)–S(1) 2.1657(9), Ni(1)–S(2) 2.1642(10), C(6)–S(1) 1.792(3), C(7)–S(2) 1.781(3), C(6)–N(3) 1.285(4), C(7)–N(4) 1.287(4), C(6)–N(5) 1.341(4), C(7)–N(6) 1.344(4), C(10)–N(1) 1.282(4), C(13)–N(2) 1.293(4), N(1)–N(3) 1.412(4), N(2)–N(4) 1.425(4); S(2)–Ru(1)–S(1) 75.14(3), S(2)–Ru(1)–Cl(1) 170.81(3), S(1)–Ru(1)–S(4) 173.59(3), S(3)–Ru(1)–Cl(2) 175.77(3), N(2)–Ni(1)–N(1) 102.08(11), S(1)–Ni(1)–S(2) 85.62(3), N(1)–Ni(1)–S(1) 83.72(8), N(2)–Ni(1)–S(2) 87.61(8), Ni(1)–S(1)–Ru(1) 87.15(3), Ni(1)–S(2)–Ru(1) 87.98(3), N(1)–Ni(1)–S(2) 168.38(8), N(2)–Ni(1)–S(1) 168.10(8).

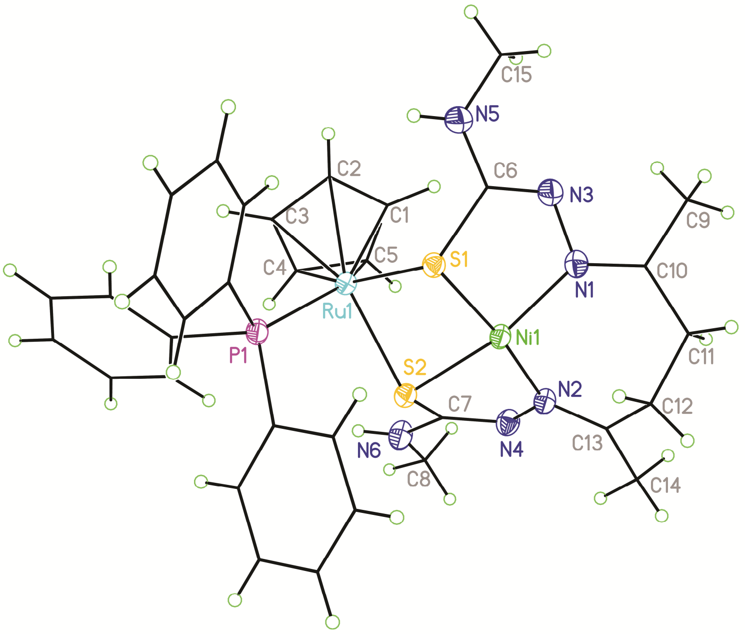

Fig. 2. Molecular structure of one anion of [CpRu{Ni(L^2-Me)}(PPh$_3$)]Cl·EtOH (**6**·EtOH), with thermal ellipsoids drawn at the 40% probability level. Solvent molecules and the counter anion are omitted for clarity. Selected bonds (Å) and angles (°): Ru(1)–S(1) 2.4570(8), Ru(1)–S(2) 2.3990(7), Ru(1)–P(1) 2.3297(8), Ru(1)–C(1) 2.187(3), Ru(1)–C(2) 2.171(3), Ru(1)–C(3) 2.157(3), Ru(1)–C(4) 2.173(3), Ru(1)–C(5) 2.192(3), Ru(1)···Ni(1) 3.116, Ni(1)–N(1) 1.952(2), Ni(1)–N(2) 1.896(2), Ni(1)–S(1) 2.1801(8), Ni(1)–S(2) 2.1656(8), C(6)–S(1) 1.791(3), C(7)–S(2) 1.798(3), C(6)–N(3) 1.288(4), C(7)–N(4) 1.307(4), C(6)–N(5) 1.343(4), C(7)–N(6) 1.333(4), C(10)–N(1) 1.301(4), C(13)–N(2) 1.286(4), N(1)–N(3) 1.418(4), N(2)–N(4) 1.411(3); S(2)–Ru(1)–S(1) 77.83(3), S(2)–Ru(1)–P(1) 88.35(3), S(1)–Ru(1)–P(1) 92.45(3), N(2)–Ni(1)–N(1) 99.46(10), S(1)–Ni(1)–S(2) 89.17(3), N(1)–Ni(1)–S(1) 87.32(8), N(2)–Ni(1)–S(2) 83.89(7), Ni(1)–S(1)–Ru(1) 84.22(3), Ni(1)–S(2)–Ru(1) 85.95(3), N(1)–Ni(1)–S(2) 164.79(8), N(2)–Ni(1)–S(1) 173.05(8).

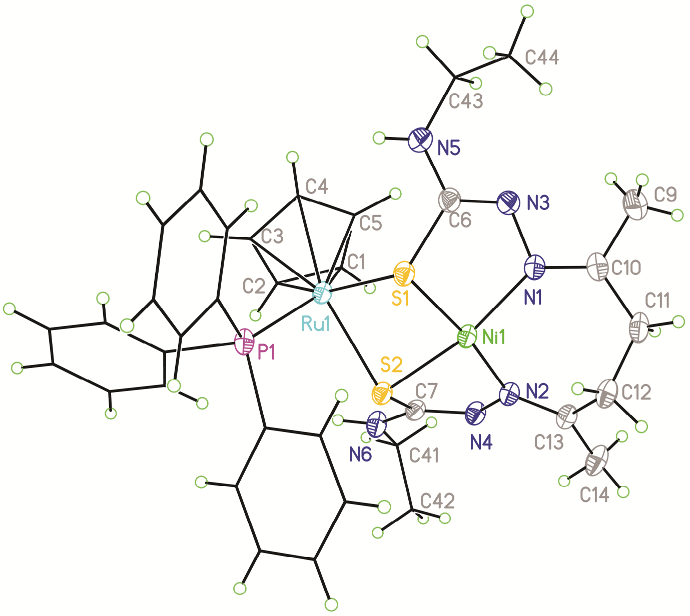

Fig. 3. Molecular structure of one anion of [CpRu{Ni(L^3-Et)}(PPh_3)]Cl·H_2O (**7**·H_2O), with thermal ellipsoids drawn at the 40% probability level. Solvent molecules and the counter anion are omitted for clarity. Selected bonds (Å) and angles (°): Ru(1)–S(1) 2.4570(6), Ru(1)–S(2) 2.4046(6), Ru(1)–P(1) 2.3327(6), Ru(1)–C(1) 2.198(3), Ru(1)–C(2) 2.173(2), Ru(1)–C(3) 2.156(2), Ru(1)–C(4) 2.169(2), Ru(1)–C(5) 2.199(3), Ru(1)$\cdots$Ni(1) 3.139, Ni(1)–N(1) 1.9554(19), Ni(1)–N(2) 1.9008(18), Ni(1)–S(1) 2.1813(6), Ni(1)–S(2) 2.1632(6), C(6)–S(1) 1.789(2), C(7)–S(2) 1.797(2), C(6)–N(3) 1.294(3), C(7)–N(4) 1.303(3), C(6)–N(5) 1.341(3), C(7)–N(6) 1.331(3), C(10)–N(1) 1.294(3), C(13)–N(2) 1.284(3), N(1)–N(3) 1.414(3), N(2)–N(4) 1.413(2); S(2)–Ru(1)–S(1) 77.48(2), S(2)–Ru(1)–P(1) 88.44(2), S(1)–Ru(1)–P(1) 92.61(2), N(2)–Ni(1)–N(1) 99.81(8), S(1)–Ni(1)–S(2) 88.91(2), N(1)–Ni(1)–S(1) 87.21(6), N(2)–Ni(1)–S(2) 83.74(6), Ni(1)–S(1)–Ru(1) 84.97(2), Ni(1)–S(2)–Ru(1) 86.65(2), N(1)–Ni(1)–S(2) 165.07(6), N(2)–Ni(1)–S(1) 172.64(6).

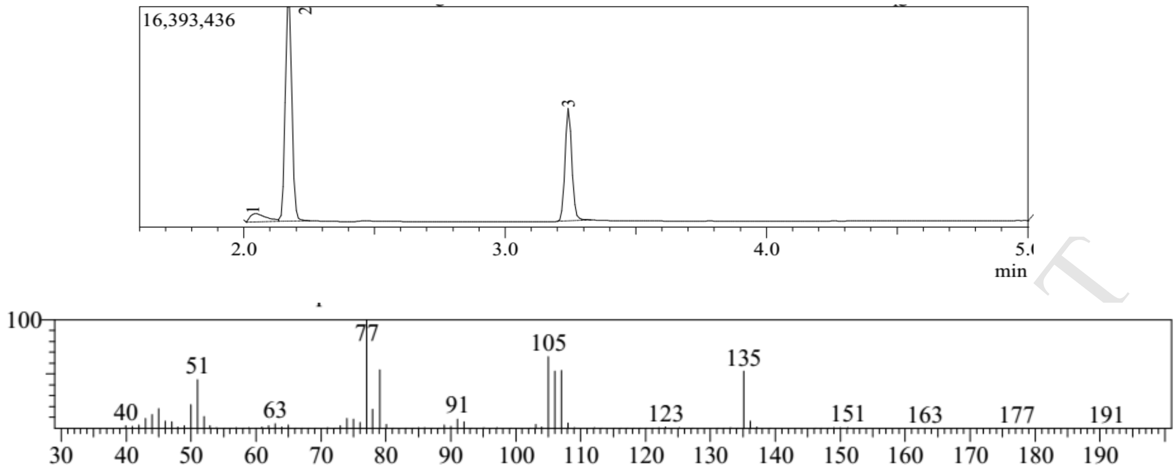

Fig. 4. Product analysis (GC-MS) from reaction of benzaldehyde and ethanol under dihydrogen catalyzed by complex $[RuCl_2\{(Ni(L^2–Me)\}(dmso)_2]$ (**2**).

For Table of Contents

Synopsis

Syntheses, characterization and reactivity of dinuclear ruthenium-nickel complexes with hexane-2,5-dione bis(thiosemicarbazonato) ligands

Duo-Wen Fang, Ai-Quan Jia*, Xian-Ping Dong, Zhifeng Xin, and Qian-Feng Zhang*

A series of bimetallic ruthenium-nickel Ni(μ-S)$_2$Ru complexes based on metalloligands hexane-2,5-dione bis(thiosemicarbazonato)nickel(II) have been synthesized and characterized, and these bimetallic ruthenium-nickel complexes could effectively catalyze acetalation of benzaldehyde with ethanol in the presence of H$_2$.

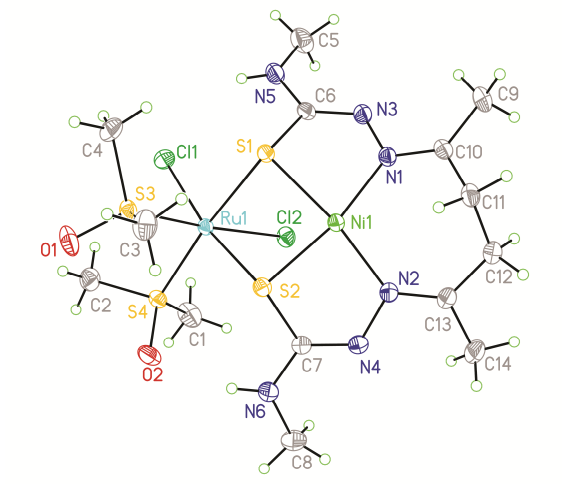

Highlights

► A series of dinuclear Ni(μ-S)$_2$Ru complexes were synthesized based on NiL^{N2S2} ligands.

► The Ni(μ-S)$_2$Ru complexes were characterized by single-crystal X-ray crystallography.

► The dinuclear Ni(μ-S)$_2$Ru complexes may catalyze acetalation of benzaldehyde with ethanol in the presence of H$_2$.